Available online at www.sciencedirect.com

ScienceDirect

Advances in Space Research 55 (2015) 2305–2314

ADVANCES IN SPACE RESEARCH (a COSPAR publication)

www.elsevier.com/locate/asr

Statistical selection of tide gauges for Arctic sea-level reconstruction

Peter Limkilde Svendsen [a,*], Ole Baltazar Andersen [a], Allan Aasbjerg Nielsen [b]

[a] *DTU Space, Technical University of Denmark, Elektrovej 328, 2800 Kgs. Lyngby, Denmark*
[b] *DTU Compute, Technical University of Denmark, Richard Petersens Plads 324, 2800 Kgs. Lyngby, Denmark*

Received 31 March 2014; received in revised form 15 January 2015; accepted 19 January 2015
Available online 2 February 2015

Abstract

In this paper, we seek an appropriate selection of tide gauges for Arctic Ocean sea-level reconstruction based on a combination of empirical criteria and statistical properties (leverages). Tide gauges provide the only in situ observations of sea level prior to the altimetry era. However, tide gauges are sparse, of questionable quality, and occasionally contradictory in their sea-level estimates. Therefore, it is essential to select the gauges very carefully.

In this study, we have established a reconstruction based on empirical orthogonal functions (EOFs) of sea-level variations for the period 1950–2010 for the Arctic Ocean, constrained by tide gauge records, using the basic approach of Church et al. (2004). A major challenge is the sparsity of both satellite and tide gauge data beyond what can be covered with interpolation, necessitating a time-variable selection of tide gauges and the use of an ocean circulation model to provide gridded time series of sea level. As a surrogate for satellite altimetry, we have used the Drakkar ocean model to yield the EOFs.

We initially evaluate the tide gauges through empirical criteria to reject obvious outlier gauges. Subsequently, we evaluate the "influence" of each Arctic tide gauge on the EOF-based reconstruction through the use of statistical leverage and use this as an indication in selecting appropriate tide gauges, in order to procedurally identify poor-quality data while still including as much data as possible.

To accommodate sparse or contradictory tide gauge data, careful preprocessing and regularization of the reconstruction model are found to make a substantial difference to the quality of the reconstruction and the ability to select appropriate tide gauges for a reliable reconstruction. This is an especially important consideration for the Arctic, given the limited amount of data available. Thus, such a tide gauge selection study can be considered a precondition for further studies of Arctic sea-level reconstruction.

Keywords: Empirical orthogonal functions; Leverage; Principal component analysis

1. Introduction

Sea-level reconstructions spanning several decades have been examined in numerous studies (Church et al., 2004; Cazenave and Le Cozannet, 2008; Calafat et al., 2014; Jevrejeva et al., 2014), typically where satellite altimetry missions such as TOPEX/Poseidon and Jason-1 and Jason-2 have provided accurate measurements of variability and long-term changes in sea level. However, these dedicated oceanographic missions are limited in coverage to between $\pm 66^{\circ}$ latitude, and satellite data at higher latitudes are of a substantially lower quality.

For sea-level reconstructions in the Arctic Ocean region, especially careful consideration needs to be given to data preprocessing, as the tide gauge data available are very limited in extent, both spatially and temporally. We specifically look at the leverage, a statistical property describing the influence upon the solution, of each individual tide gauge. We examine the appropriateness of removing high-leverage gauges (gauges that have the highest influence) from the

* Corresponding author. Tel.: +45 45259742; fax: +45 45259575.
E-mail addresses: plsv@space.dtu.dk (P.L. Svendsen), oa@space.dtu.dk (O.B. Andersen), alan@dtu.dk (A.A. Nielsen).

http://dx.doi.org/10.1016/j.asr.2015.01.017
0273-1177/

data, and the qualitative consequences on the reconstruction.

For global sea-level reconstructions, a common procedure is to constrain the reconstruction using a limited number of high-quality gauges, under criteria such as length of time series and geodynamic stability; see, for example, Douglas (1997). To avoid manual editing of the data, and because there are so few gauges to choose from, we seek to establish appropriate criteria for tide gauge inclusion. We consider only per-gauge criteria, not assessment of individual observations.

Achieving full spatial coverage in the reconstruction is typically done by extracting the leading empirical orthogonal functions (EOFs) from an altimetry dataset, which then serves as calibration for the reconstruction. However, as Arctic altimetry data are limited in a spatial extent and has seasonally variable availability, we use data from the Drakkar ocean model (Barnier et al., 2006).

As this paper is intended as a preliminary study towards an altimetry-based reconstruction, we have used only the Drakkar data from within the altimetry era. This has a small effect on the appearance of the EOFs.

We derive and compare three sea-level reconstructions for the Arctic Ocean for the period 1950–2010: one including all available gauges above 68°N with at least 5 years of data in the reconstruction period 1950–2010 (excluding data flagged in the dataset as having poor quality), one with empirically conspicuous (high sea-level trend) gauges removed, and one in which high-leverage gauges are also removed. Additionally, comparison is made with a reconstruction using only a spatially uniform pattern (the "EOF0").

2. Data

The EOFs for the calibration period were obtained from the Drakkar ocean model (Barnier et al., 2006), spanning the period 1958–2007. Prior to EOF computation, the model grids have been spatially and temporally limited so as to only include data above 68°N, and to cover only the period from 1993 (in order to simulate the availability of satellite altimetry). We have chosen the cutoff latitude at 68°N to avoid artifacts from the Baltic Sea.

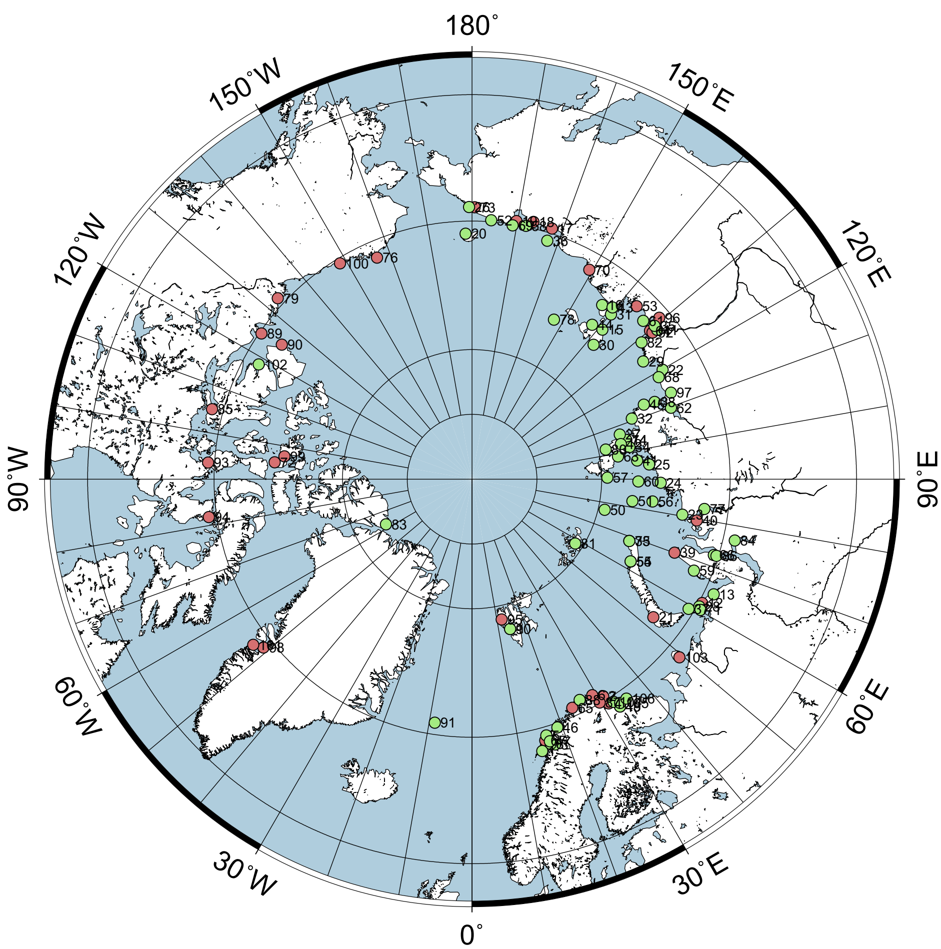

Fig. 1. All 106 PSMSL tide gauges above 68°N. Green dots mark the 69 gauges with at least 5 years of data and trends within ±2 cm/year, while red dots mark rejected gauges. The gauges are labelled with numbers 1–106, a numbering particular to this selection of Arctic gauges.

The reconstruction uses tide gauge data from the Permanent Service for Mean Sea Level (PSMSL) database (Holgate et al., 2012; Permanent Service for Mean Sea Level (PSMSL), 2014). The lengths of PSMSL records in the Arctic are substantially limited compared to those used in global reconstructions. For many gauges along the northern coast of Siberia, there are data records available only in the approximate period 1960–1990, unfortunately precluding an overlap with satellite data that would have aided in setting up and validating our reconstruction.

The PSMSL database contains both “metric-only” and, where a reasonable vertical reference can be determined, “Revised Local Reference” (RLR) records. In some cases, only metric data are available; in the case of the Arctic Ocean, gauges with only metric data are concentrated largely around Greenland and Canada. While great caution is advised when using metric-only data, we do allow it (as in Church et al., 2004) as we use height *changes* (first differences) in the time series. Gauges and observations with quality flags in the PSMSL records have been removed, which should eliminate the most substantial datum shifts.

There are a total of 106 PSMSL gauges above 68° N, the spatial distribution of which is shown in Fig. 1. The number of gauges fulfilling our various inclusion criteria are listed in Table 1. The availability of tide gauge data over time is shown in Fig. 2. It is readily apparent that there is a clear dominance of Russian and Norwegian gauges, and a very substantial loss of Russian gauges around 1990.

Correction for glacial isostatic adjustment (GIA) has been applied to the tide gauge data, using the Peltier dataset with ICE-5G deglaciation history (Peltier, 2004). Using 14 different GIA models, Huang et al., 2013 found a relatively large range of GIA trends for tide gauges, but a relatively small contribution range of between −0.24 and 0.11 mm/year to any potential altimeter-measured sea level between 66°N and 90°N.

Prior to the reconstruction, we apply an inverse barometer (IB) correction to the tide gauge records to make them comparable to the Drakkar data. The pressure data are obtained from the Hadley Centre Sea Level Pressure (HadSLP2) dataset ($5 \times 5^\circ$ monthly grids; Allan and Ansell, 2006) and interpolated to the individual tide gauge locations. The pressure-driven contribution is applied using anomalies from the local pressure mean over the reconstruction period. It should be noted that the HadSLP2 data are themselves based on reduced-space optimal interpolation, and therefore include a substantial amount of reconstructed values.

Some Arctic gauges exhibit extraordinary trends, in some cases 0.5–1 m/year. Regional sea-level trends have been estimated to be in the range of approximately −2 cm/year to +2cm/year (Nerem et al., 2006). Therefore, to ensure basic plausibility, gauges with estimated trends outside a particular range have been removed in preprocessing. Based on the analysis in Section 4.1, we reject gauges with trends larger than ±2 cm/year (after GIA and IB correction). Gauges with <5 years of data available within our reconstruction period are also removed in this

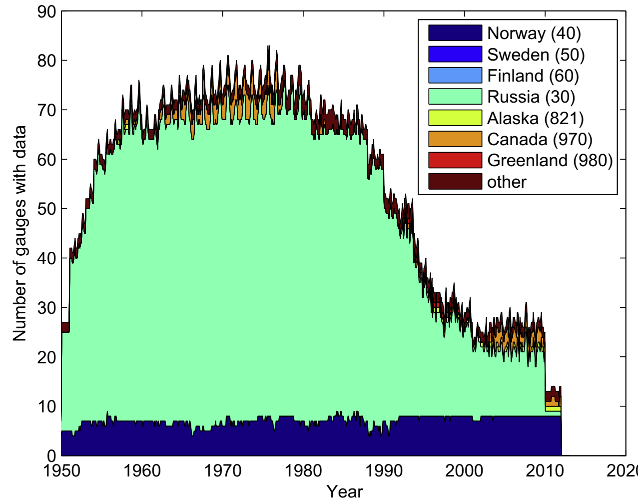

Fig. 2. Availability of data for the gauges above 68°N by coastline. Numbers in parentheses indicate PSMSL coastline IDs.

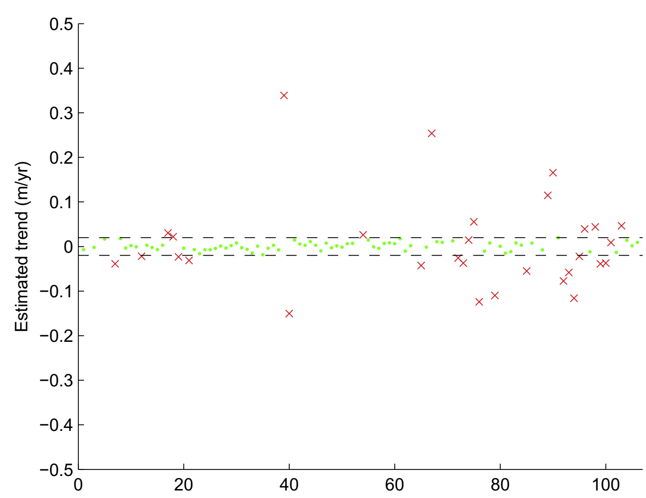

Fig. 3. Trends for each of the 106 Arctic tide gauges. The 69 gauges falling within ±2 cm/year and at least 5 years of data are shown in green, whereas those rejected on either criterion are shown in red. The gauges are numbered 1 through 106 as in Fig. 1. Note that three gauges are outside (below) the vertical range of the plot. (For interpretation of the references to colour in this figure legend, the reader is referred to the web version of this article.)

Table 1
Number of available gauges corresponding to different inclusion criteria.

Inclusion criteria	No. gauges
Above 68°N	106
At least 5 years of data in reconstruction period	90
Trend within ±2 cm/year and ⩾ 5 year data in reconstruction period	69
The above and “moderate” leverage	67

preprocessing. An overview of the trends of the gauges is shown in Fig. 3.

For comparison, Church et al., 2004 removed continuous sections shorter than 2 years and removed gauges deemed unsuitable (such as in estuaries and if contradicting nearby gauges, having noisy time series, or having a residual trend of >1 cm/year). However, for the sparse Arctic data, a fairly inclusive approach is needed.

In a Russian-sector study of tide gauge trends between 1954 and 1989, Proshutinsky et al. (2004) required near-completeness of the time series, allowing a maximum of 10 missing months from each time series in that period. However, we aim to reconstruct the largest spatial and temporal range possible for the Arctic Ocean, rather than achieving great robustness for a particular area.

In establishing a global sea-level reconstruction, Meyssignac et al. (2012) carefully picked 91 gauges across the globe. Those gauges were chosen using more elaborate (and stringent) criteria than have been applied here, including only RLR data, requiring at least 35 years of data in the time series, and omitting outlier gauges based on Rosner's test (Rosner, 1975), which is aimed at detecting outliers even when they may be masked by other outliers.

3. Reconstruction method

The reconstruction is based on the method from Church et al. (2004). That is, the spatial (EOF) patterns from a calibration period are used in conjunction with tide gauge records to yield a reconstruction covering the timespan of the tide gauges. In this case, the EOFs are obtained from Drakkar fields.

With this reconstruction method, the oceans are assumed to have a stationary covariance pattern, derived from the Drakkar model grids. From these, the first few EOFs are determined. The EOFs are amended with a spatially uniform pattern to capture any overall trend; this uniform pattern is commonly known as "EOF0." The first eight EOFs (in addition to the EOF0) are retained in the basis of our reconstruction; see the analysis section. Calafat et al. (2014) argued that regional variability is better captured in global sea-level reconstructions if the EOF0 is omitted; however, we are interested in obtaining MSL trends and therefore include the EOF0.

Both the calibration (Drakkar) and tide gauge data are preprocessed to remove a constant term, as well as whole- and half-year harmonic oscillation. Unlike Church et al. (2004), no trend is removed, as the tide gauge time series are often very short, and any trend should be reasonably captured by the EOF0. The oscillations are then added back to the solution after solving for the EOF coefficients. In order to handle the unknown vertical datum of the tide gauges, first differences of their time series are used (minus the estimated relative sea-level (RSL) contribution from the GIA model), and the subsequent EOF fit temporally cumulated to provide the actual sea-level reconstruction.

To accommodate sparse or contradictory tide gauge data, the problem is regularized as described by Kaplan et al. (2000). This involves damping the influence of EOFs with small corresponding eigenvalues. As EOF0 has no inherent eigenvalue, here, it is assigned the same "eigenvalue" as EOF1. The optimal interpolation requires an error estimate, and a standard deviation of 3 cm on the tide gauge data is assumed in this case. The model lets a gauge enforce the nearest (great-circle distance) pixel in the grid, with a cutoff threshold distance of 500 km. For their global sea-level reconstruction, Church et al. (2004) allowed a maximum of 250 km between the tide gauge and the nearest altimetry grid point.

Our reconstruction uses a time-variable selection of gauges. This causes the reconstruction to be less skillful than with a constant tide gauge selection (Calafat et al. (2014)), but the sparsity of Arctic tide gauge data leaves little choice.

3.1. Optimal interpolation

The reconstruction method in Church et al. (2004) and Christiansen et al. (2010) uses optimal interpolation (OI), minimizing the cost function (in the notation of Christiansen et al. (2010)):

$$(\mathbf{HE}\boldsymbol{\alpha} - \mathbf{G})^{\mathsf{T}}\mathbf{R}^{-1}(\mathbf{HE}\boldsymbol{\alpha} - \mathbf{G}) + \boldsymbol{\alpha}^{\mathsf{T}}\boldsymbol{\Lambda}^{-1}\boldsymbol{\alpha}$$

in which $\mathbf{E}$ is the retained eigenfunctions of the calibration period, $\mathbf{G}$ is the data matrix of tide gauge heights, $\mathbf{H}$ is an indicator matrix for the positions of the tide gauges, $\mathbf{R}$ is the error covariance matrix, $\boldsymbol{\Lambda}$ is the diagonal matrix of retained eigenvalues, and $\boldsymbol{\alpha}$ is the time series (for which we are solving) corresponding to each eigenfunction. The solution for $\boldsymbol{\alpha}$ is then given by

$$\boldsymbol{\alpha} = \mathbf{PE}^{\mathsf{T}}\mathbf{H}^{\mathsf{T}}\mathbf{R}^{-1}\mathbf{G}$$

with $\mathbf{P} = (\mathbf{E}^{\mathsf{T}}\mathbf{H}^{\mathsf{T}}\mathbf{R}^{-1}\mathbf{HE} + \boldsymbol{\Lambda}^{-1})^{-1}$.

3.2. Leverage

A multivariate least-squares regression is described by the equation

$$\mathsf{y} = \mathsf{X}\boldsymbol{\theta} + \mathsf{e}$$

where y is the response variable (here, tide gauge readings), X is our predictor, $\boldsymbol{\theta}$ the model parameters, and e the residuals. We solve for $\boldsymbol{\theta}$. The so-called "hat matrix" relates the y to its estimate, $\hat{\mathsf{y}}$:

$$\hat{\mathsf{y}} = \mathsf{X}\hat{\boldsymbol{\theta}}_{OLS} = \mathsf{X}(\mathsf{X}^{\mathsf{T}}\mathsf{X})^{-1}\mathsf{X}^{\mathsf{T}}\mathsf{y}$$

The diagonal elements of $\mathsf{X}(\mathsf{X}^{\mathsf{T}}\mathsf{X})^{-1}\mathsf{X}^{\mathsf{T}}$ give the leverages of the respective observations.

For our OI fit, we estimate the leverage as the diagonal elements of the matrix

$$\mathbf{HEPE}^{\mathsf{T}}\mathbf{H}^{\mathsf{T}}\mathbf{R}^{-1}$$

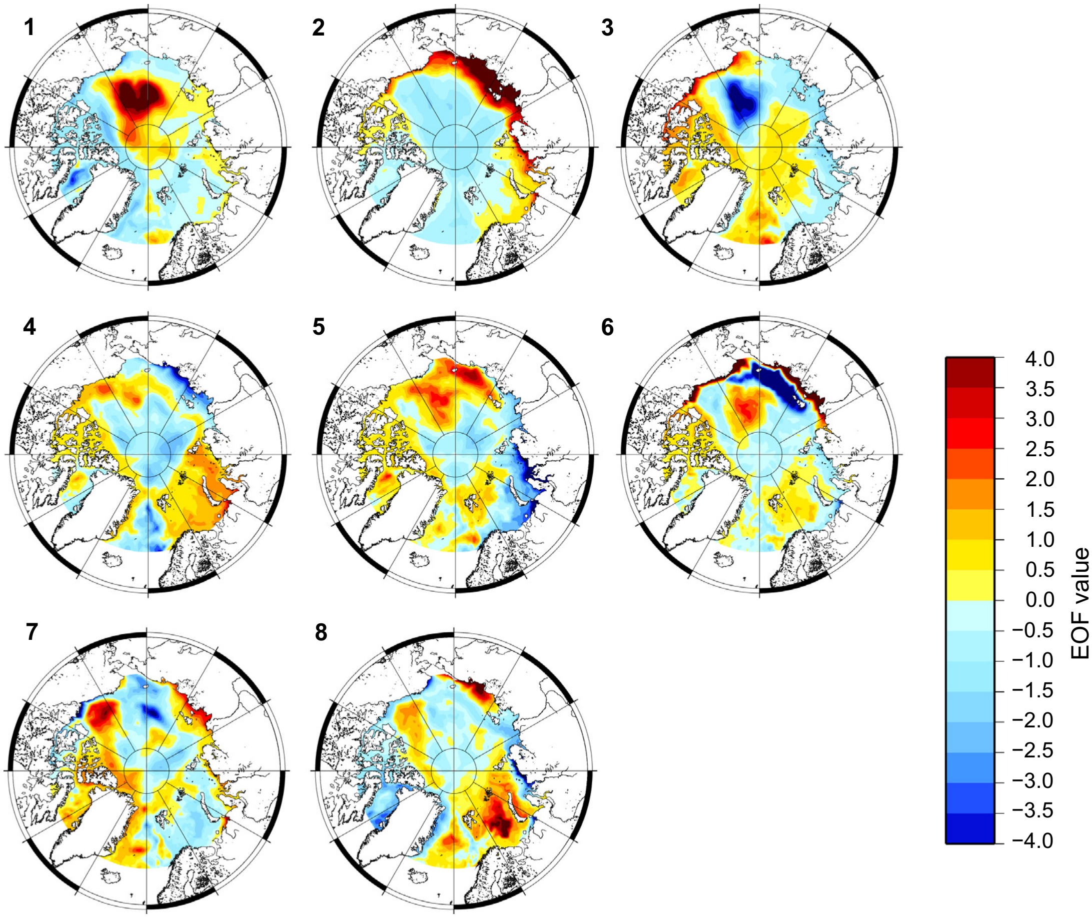

Fig. 4. The leading eight EOF patterns of the Drakkar data for the period 1993–2007 (arbitrary scaling). Note that the reconstruction includes an additional, uniform pattern, the EOF0.

Unlike in the ordinary least squares (OLS) case, the sum of the leverages will not generally equal the number of parameters. We normalize our leverage values in this case so that the leverage values for each time step sum to the same value. Note that as the normalized leverage for each gauge will vary with time and occasionally be missing (due to missing data), we estimate, for each gauge, a mean value based on the available data.

Systematic deviations from the fit can be identified using residual analysis.

4. Analysis

The leading EOF patterns of the Drakkar data are shown in Fig. 4. The dominant mode of variability (>75% explained variance) is a dipole of deep ocean versus coastal areas north of Siberia, as seen in EOF1. The corresponding time series for the patterns are shown in Fig. 5. The inclusion of eight EOFs (in addition to the EOF0) is chosen so that >95% of the Drakkar variance is explained, but only just (so as to avoid overfitting).

Including only altimetry-era data slightly affects the appearance of the EOFs, in particular the relative dominance of the Beaufort Gyre in EOF1. If using the full Drakkar dataset (1958–2007), the EOF1 pattern will be more positive in the North Atlantic and the Baffin Bay.

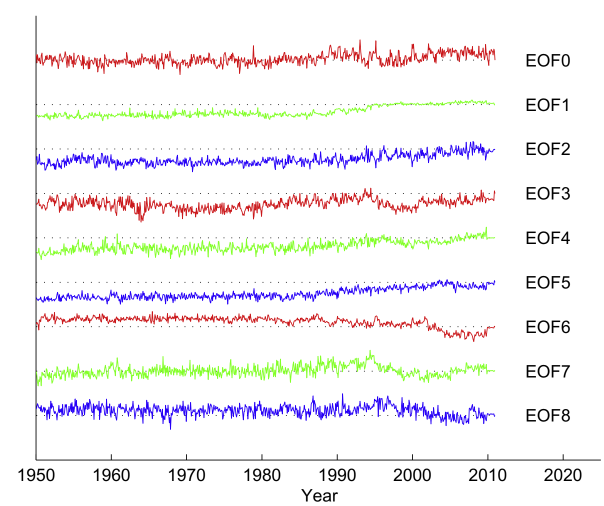

Fig. 5. Time series for the eight EOFs (and EOF0) as determined by the reconstruction including 69 gauges. The vertical scale is normalized to give them identical variance, showing in a qualitative way the nature of temporal variation.

Table 2
Reconstruction MSL trends and number of available gauges corresponding to different inclusion criteria. MSL trends are for the entire reconstruction period, 1950–2010.

Inclusion threshold	MSL trend (mm/year)	MSL trend, EOF0 only (mm/year)	Number of gauges
±1 cm/year	3.8 ± 0.3	2.3 ± 0.3	49
±2 cm/year	2.3 ± 0.3	1.0 ± 0.3	69
±3 cm/year	-1.5 ± 0.4	0.5 ± 0.3	75

The choice not to detrend the calibration data prior to the EOF analysis affects the appearance of the EOFs; the prominent Beaufort Gyre feature in EOF1 is much less apparent in the patterns if the Drakkar data are detrended first, suggesting a fairly clear trend in this area. Apart from this, a Russian-sector coastal feature dominates the variability, whether the data are detrended or not. If detrending is applied, the EOF1 is less dominant, explaining only about 51% of the variance, while the Beaufort Gyre appears mostly in EOF3. This indicates that much of the trend occurs in the pattern described by EOF1.

4.1. Trend threshold for inclusion

As a simple sanity check of the tide gauges, we set a threshold for a tolerable trend in their time series. We compute this trend by taking the mean of the month-to-month differences. Specifically, when the trend threshold is set at ±2 cm/year (see below for justification), we reject the gauge if the mean value of its month-to-month differences is larger than $\pm\frac{1}{6}\,cm$.

The overall characteristic of the reconstructed mean sea level is sensitive to the choice of trend threshold in the preprocessing step, with dramatic consequences if the threshold is set larger than a few centimeters per year. To illustrate, we have performed the reconstruction with gauge mean trend threshold set at 1, 2, and 3 cm/year, respectively. From this, we obtain the number of gauges shown in Table 2, with a corresponding MSL trend for the reconstruction. While the trend is significantly lower with the threshold at $\pm 2cm/year$ rather than ±1 cm/year, the overall character of the MSL curve is still retained (see Fig. 6) while including 20 more gauges. Increasing the threshold to ±3 cm/year introduces large vertical jumps around 1988 and 1992, and strongly disturbs the MSL trend, while only admitting six more gauges. On that basis, we have picked ±2 cm/year as the threshold that provides the best compromise between including as much data as possible and retaining a stable reconstruction.

Using a simplified reconstruction including only the EOF0 avoids the vertical jumps around 1990 (see Fig. 7) and yields more moderate MSL trends (cf. Table 2). This suggests that the reconstruction is sensitive to the decline in the number of Russian gauges when using the full set of EOFs. Otherwise, the reconstructed MSL exhibits a similar peak in the early 1990s, and a subsequent rise, both with and without EOF1–8.

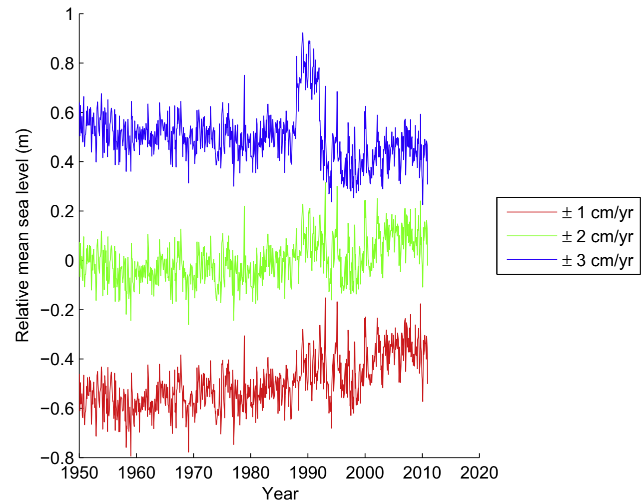

Fig. 6. Reconstructed mean sea level for the entire Arctic (above 68°N), with arbitrary vertical offsets, for different trend thresholds.

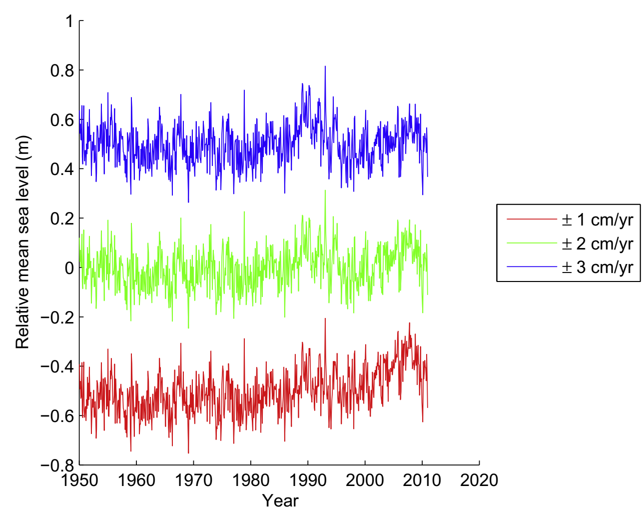

Fig. 7. Reconstructed mean sea level for the entire Arctic (above 68°N), with arbitrary vertical offsets, for different trend thresholds, using only EOF0.

4.2. Identification of influential tide gauges

The mean leverage for each included gauge is visualized in Fig. 8. It is seen that the high-leverage gauges are concentrated largely around the East Siberian Sea, although the Svalbard gauge (Barentsburg) is also estimated to be highly influential. The Barentsburg gauge is relatively geo-

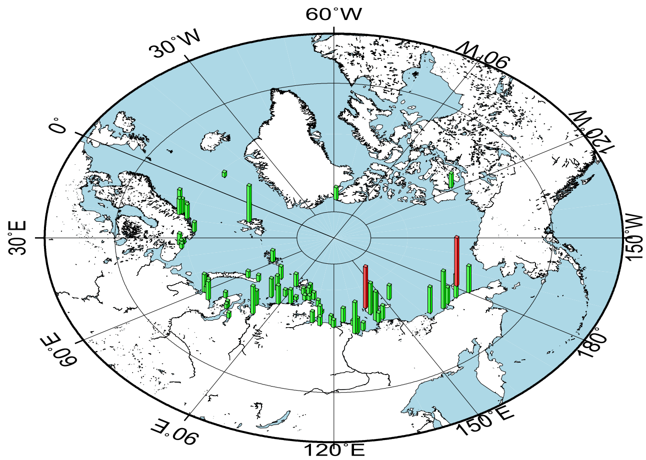

Fig. 8. Mean leverages of included gauges, shown as column height. The two highest-leverage gauges, PSMSL 608 (Vrangelia) and PSMSL 641 (Kotelnyi), are highlighted in red (right and left, respectively).

graphically isolated, and it may simply be an outlier because of that. Therefore, this gauge can be considered for inclusion despite having high leverage.

The leverage values given in this section are the mean leverages for the gauges, scaled so that 1 is equivalent to the mean "mean leverage" across the included gauges. As a rule of thumb, leverages of more than approximately three times the mean of all leverages may be considered suspicious (Nielsen, 2013), although not necessarily inappropriate for inclusion in the reconstruction. The highest and lowest leverage values for the gauges are shown in Tables 3 and 4, respectively.

The reconstructed sea level for the five highest-leverage gauges is shown in Fig. 9. It seems that there is a qualitatively reasonable agreement between the reconstruction and both tide gauge and calibration data; however, a rather large vertical gap seems to develop for the two first stations (Vrangelia and Kotelnyi, PSMSL codes 608 and 641, respectively) around 2000. Therefore, the high leverage could be due to a mismatch in trend between the tide gauge record and the reconstructed sea level at its location, which could possibly be attributed to GIA uncertainties. Based on the appearance of these two time series, and their leverage being around three times the gauge mean or higher (with a small downward jump between these two gauges and that of the third; see Fig. 10), we consider these two gauges to be rejectable. Their geographical locations are highlighted in Fig. 8.

Omission of the two high-leverage gauges very slightly increases the overall MSL trend for the Arctic in the period 1950–2010. However, the resulting trend is 2.3 mm/year, <0.1 mm/year different from a reconstruction with the gauges included, which is not statistically significant (see Table 2).

4.3. Correspondence with previous studies

Examining the Norwegian and Russian sectors from 1950, Henry et al., 2012 found no significant trend in coastal sea level for the period 1950–1980, but an increasing trend since 1980, and a post-1995 trend of approximately 4 mm/year. Our reconstructed (relative)

Table 3
Tide gauges having the highest leverage (strong-trend gauges having been rejected in preprocessing).

Rank	PSMSL ID	Arctic gauge No.	Name	Mean leverage (normalized)
1	608	20	VRANGELIA	3.54
2	641	30	KOTELNYI	3.03
3	730	58	AION	2.74
4	541	9	BARENTSBURG	2.66
5	569	11	TIKSI	2.29
6	602	15	SANNIKOVA	2.28
7	642	31	KIGILIAH	2.09
8	917	77	SOPOCHNAIA KARGA	2.02
9	616	26	MYS SHMIDTA	1.93
10	650	36	CHETYREHSTOLBOVOI	1.90

Table 4
Tide gauges having the lowest leverage (strong-trend gauges having been rejected in preprocessing).

Rank	PSMSL ID	Arctic gauge No.	Name	Mean leverage (normalized)
60	1019	82	SAGYLLAH-ARY	0.36
61	2028	106	TERIBERKA	0.35
62	687	49	MURMANSK II	0.35
63	601	14	FEDOROVA	0.34
64	1200	86	SE-LAHA	0.33
65	1382	91	JAN MAYEN	0.32
66	531	8	EVENSKJAER	0.28
67	655	41	RUSSKII	0.25
68	2026	104	MYS PIKSHUEVA	0.24
69	667	45	MARII PRONCHISHEVOI	0.20

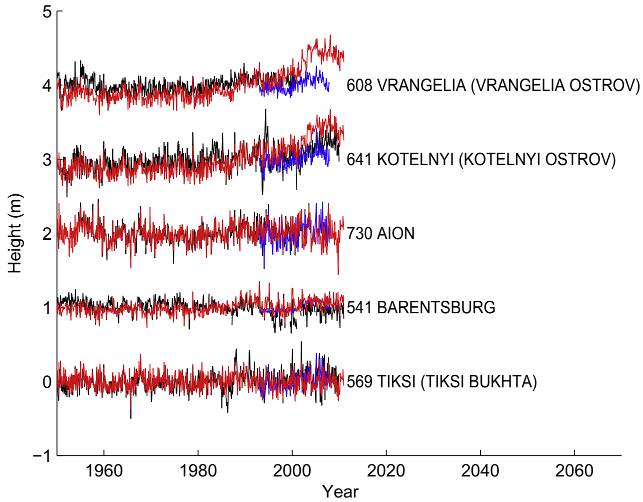

Fig. 9. Measured (black) and reconstructed (red) time series for the highest-leverage gauges, along with the corresponding Drakkar data (blue). (For interpretation of the references to colour in this figure legend, the reader is referred to the web version of this article.)

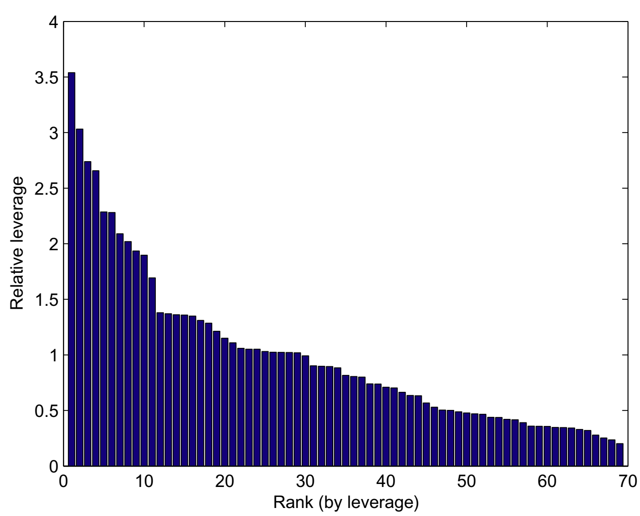

Fig. 10. Leverages of the 69 gauges that fulfil the empirical criteria (see Table 1), sorted by descending leverage.

mean sea level for the Arctic Ocean generally shows similar results (see Fig. 11 and Table 5), albeit with substantial high-frequency variation. It is notable that there is a clear, sudden rise around 1990 when including all gauges, which is virtually absent if the ± 2 cm/year trend and record length criteria are applied.

Giles et al., 2012 found, using satellite measurements from the period 1995–2010, a distinct increasing trend in freshwater storage (and associated increase in sea surface height of 18.8 ± 0.9 mm/year) in the Western Arctic Ocean around the Beaufort Gyre, starting around 2002. Specifically, the study refers to an area between 180° and 130°W; our resulting trends for the same area are given in Table 6. While simply including all gauges with a reasonable amount of data yields a similar increase in trend around 2002, a sea-level rise is also seen with our other

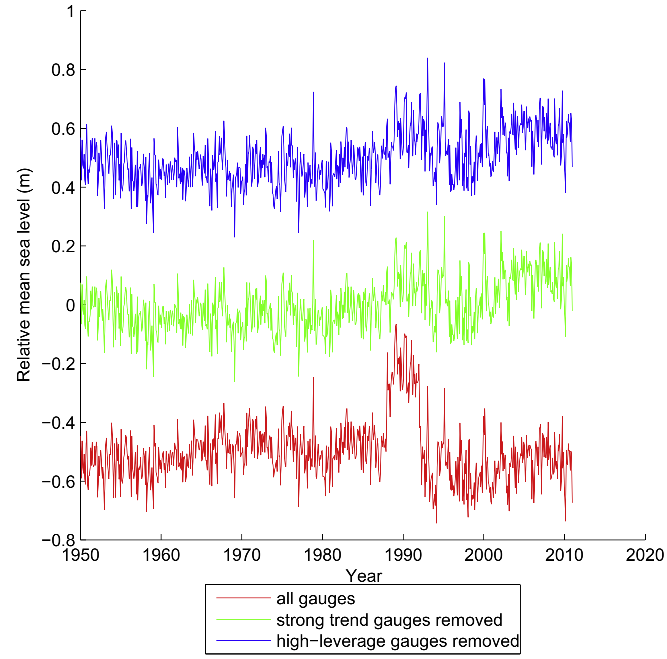

Fig. 11. Reconstructed mean sea level for the Arctic Ocean (above 68°N), with arbitrary vertical offsets.

Table 5
Mean sea-level trends in the Arctic Ocean for reconstructions based on different selections of tide gauges.

Inclusion criteria	Trend 1950–1980 (mm/year)	Trend 1980–2010 (mm/year)
$\geqslant$ 5 years of data in time span	2.7 ± 0.8	-4.6 ± 1.4
Trend within ± 2 cm/year and $\geqslant$ 5 year data	-0.5 ± 0.8	4.0 ± 1.0
The above and “moderate” leverage	-0.6 ± 0.8	3.8 ± 1.0

selections of gauges; the increase merely happens earlier. It should be noted that the study by Giles et al. (2012) is based on altimetry, whereas our reconstructions use Drakkar model data and only a single Canadian-sector gauge. Our reconstructed MSL for the area is shown in Fig. 12; note the larger trend in 1950–1970 when empirical removal of gauges is not performed. A large sea-level increase in the Amerasian basin (comprising the Canada and Makarov Basins) in 2003–2009 has also been found by Koldunov et al. (2014).

The complete lack of tide gauge coverage of the deeper parts of the Arctic Ocean represents a major difficulty, and the sea level in the deep basins may not necessarily correlate well with that in shelf areas.

4.4. Correspondence between data and reconstruction

The root-mean-square error (RMSE) between reconstructed and observed sea level at the location of each of the 106 tide gauges above 68°N is shown in Fig. 13 (of which only 69 gauges have been determined as appropriate

Table 6
Mean sea-level trends in Western Arctic Ocean (130° W to 180° W) for reconstructions based on different selections of tide gauges.

Inclusion criteria	Trend 1950–2010 (mm/year)	Trend 1996–2002 (mm/year)	Trend 2002–2010 (mm/year)
$\geqslant$ 5 years of data in time span	10.2 ± 0.5	5.3 ± 10.1	9.8 ± 6.4
Trend within ± 2 cm/year and $\geqslant$ 5 year data	5.8 ± 0.4	21.5 ± 10.1	-4.3 ± 5.8
The above and "moderate" leverage	6.5 ± 0.4	23.8 ± 10.1	-4.6 ± 5.8

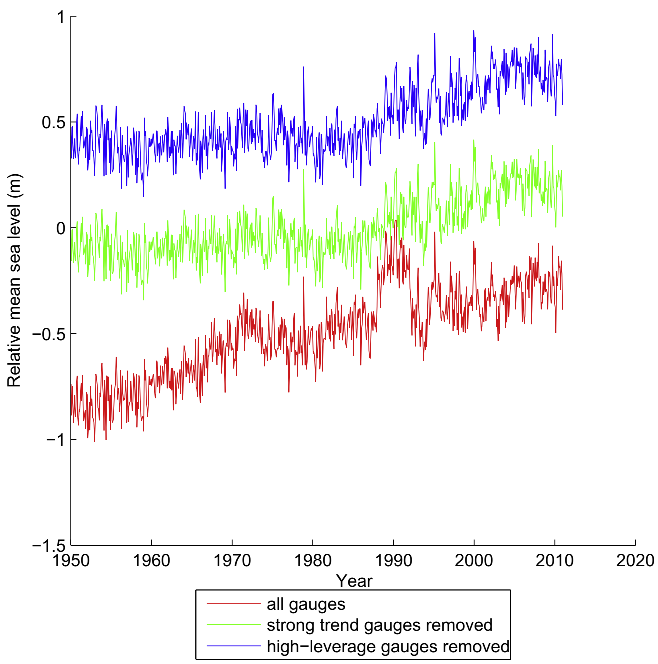

Fig. 12. Reconstructed mean sea level for the Western Arctic Ocean (longitudes 130°W to 180°W), with arbitrary vertical offsets.

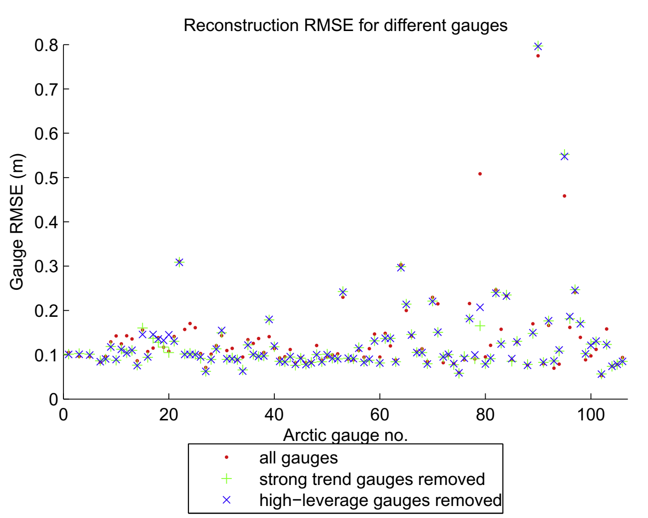

Fig. 13. RMSE for reconstruction versus tide gauge records for reconstructions based on different selections of tide gauges.

for driving the reconstruction). Four of the 106 gauges have insufficient data in the reconstruction period to compute an RMSE relative to the observed data, and the RMSE values are thus computed for only 102 gauges.

The mean RMSE across the 102 Arctic gauges is 0.137 m when all gauges with at least 5 years of data are included, 0.128 m when an empirical gauge removal has been done, and 0.129 m when the two high-leverage gauges are removed. Although the RMSE increases slightly on average by omitting these two gauges, it must be noted that the empirical gauge removal lowers the RMSE for 63 of the 102 gauges, and omitting the two gauges further lowers the RMSE for 60 gauges.

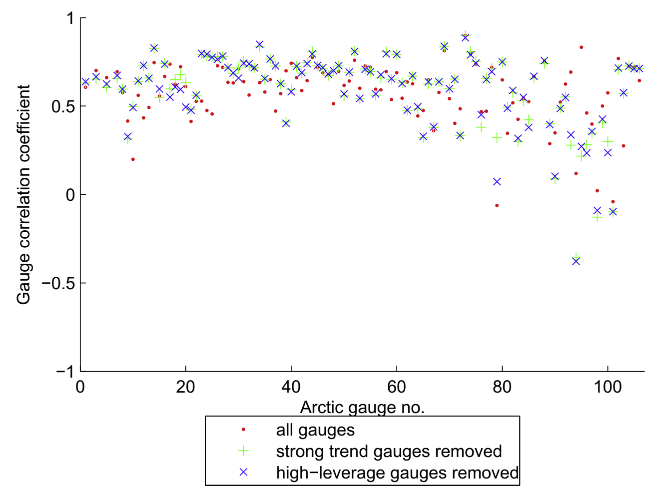

Fig. 14. Correlation coefficients for reconstruction versus tide gauge records for reconstructions based on different selections of tide gauges.

The correlation coefficients for the reconstructed time series versus the recorded time series of the Arctic gauges are shown in Fig. 14. The mean of the correlation coefficients across the gauges is 0.575 when all gauges with enough data, 0.592 when removing high-trend gauges, and 0.588 when removing the two high-leverage gauges.

The fit is slightly poorer on average when omitting the high-leverage gauges. However, removing the high-trend gauges improves correlation for 62 of the 102 gauges and removing the high-leverage gauges further improves it for 61 gauges.

When performing the reconstruction with the high-trend gauges removed, three gauges (1419 Igloolik, 1820 Ilulissat and 1900 Aasiaat) exhibit a negative correlation coefficient; all of these are metric-only gauges.

5. Conclusions

Our reconstruction approach allows tide gauges with substantial gaps in their time series to be used in the reconstruction, in contrast to requiring near-complete records throughout the reconstruction time span. This is an important necessary difference with global sea-level reconstructions, where such demands can more easily be made. The reconstruction is very sensitive to tide gauge selection, as small changes to inclusion criteria can result in large changes to reconstructed sea-level trends.

We estimate the overall trend for the Arctic MSL at approximately 2.3 ± 0.3 mm/year for the period 1950–2010, with a post-1980 trend of approximately 3.8 ± 1.0 mm/year. However, these values are highly sensitive to the inclusion criteria applied to the gauges, and also whether the reconstruction is based the full set of EOFs or only the EOF0.

Using only the EOF0 in the reconstruction appears to improve the robustness of the reconstruction. However, much of the expected sea-level rise is confined to the Beaufort Gyre, and inclusion of EOFs to capture this local trend is attractive, assuming it can be adequately controlled. This is a difficult issue as this mode of variability (captured in EOF1) has little expression in the coastal areas where the tide gauges are located.

While the selection of tide gauges seems to be key in providing a good reconstruction, statistical leverage appears useful in identifying outlier gauges, allowing further refinement of the reconstruction. Based on the present study, leverage seems to help in identifying data where trend estimates are inconsistent with the surrounding area, although less useful in identifying poor-quality data. Trend inconsistencies are an important phenomenon in the Arctic, where GIA is generally not well constrained. Removing the high-leverage gauges also results in better correspondence between reconstruction and tide gauge records for the vast majority of tide gauges.

Our reconstruction appears consistent with previous studies, including a distinctive increase in sea-level trend around 1980 as found by Henry et al., 2012, and an increase in sea level for the western Arctic Ocean since the early 1990s as described by Giles et al., 2012, although the timing of the latter is rather dependent on the gauge inclusion criteria.

Acknowledgments

We thank the anonymous reviewers for their constructive comments, which have provided many valuable improvements to the article.

References

Allan, R., Ansell, T., 2006. A new globally complete monthly historical gridded mean sea level pressure dataset (HadSLP2): 1850-2004.

Barnier, B., Madec, G., Penduff, T., Molines, J.-M., Treguier, A.-M., Le Sommer, J., Beckmann, A., Biastoch, A., Boening, C., Dengg, J., Derval, C., Durand, E., Gulev, S., Remy, E., Talandier, C., Theetten, S., Maltrud, M., McClean, J., De Cuevas, B., 2006. Impact of partial steps and momentum advection schemes in a global ocean circulation model at eddy-permitting resolution. Ocean Dyn. 56 (5–6), 543–567.

Calafat, F.M., Chambers, D.P., Tsimplis, M.N., 2014. On the ability of global sea level reconstructions to determine trends and variability. J. Geophys. Res. Oceans 119, 1572–1592. http://dx.doi.org/10.1002/2013JC009298.

Cazenave, A., Le Cozannet, G., 2008. Sea level rise and its coastal impacts. Earth's Future 2 (2), 15–34. http://dx.doi.org/10.1002/2013EF000188.

Christiansen, B., Schmith, T., Thejll, P., 2010. A surrogate ensemble study of sea level reconstructions. J. Clim. 23 (16), 4306–4326.

Church, White, Coleman, Lambeck, Mitrovica, 2004. Estimates of the regional distribution of sea level rise over the 1950-2000 period. J. Clim. 17 (13), 2609–2625.

Douglas, B.C., 1997. Global sea rise: a redetermination. Surv. Geophys. 18 (2–3), 279–292.

Giles, K.A., Laxon, S.W., Ridout, A.L., Wingham, D.J., Bacon, S., 2012. Western arctic ocean freshwater storage increased by wind-driven spin-up of the Beaufort Gyre. Nat. Geosci. 5 (3), 194–197.

Henry, O., Prandi, P., Llovel, W., Cazenave, A., Jevrejeva, S., Stammer, D., Meyssignac, B., Koldunov, N., 2012. Tide gauge-based sea level variations since 1950 along the Norwegian and Russian coasts of the Arctic Ocean: contribution of the steric and mass components. J. Geophys. Res.: Oceans, 117.

Holgate, S.J., Matthews, A., Woodworth, P.L., Rickards, L.J., Tamisiea, M.E., Bradshaw, E., Foden, P.R., Gordon, K.M., Jevrejeva, S., Pugh, J., 2012. New data systems and products at the permanent service for mean sea level. J. Coastal Res. 29 (3), 493.

Huang, Z., Guo, J.-Y., Shum, C.K., Wan, J., Duan, J., Fok, H.S., Kuo, C.-Y., 2013. On the accuracy of glacial isostatic adjustment models for geodetic observations to estimate Arctic Ocean sea-level change. Terr. Atmos. Oceanic Sci. 24 (4), 471–490. http://dx.doi.org/10.3319/TAO.2012.08.28.01(TibXS.

Jevrejeva, S., Moore, J., Grinsted, A., 2014. Trends and acceleration in global and regional sea levels since 1807. Global Planet. Change 113, 11–22.

Kaplan, A., Kushnir, Y., Cane, M.A., 2000. Reduced space optimal interpolation of historical marine sea level pressure: 1854–1992. J. Clim. 13 (16), 2987–3002.

Koldunov, N.V., Serra, N., Köhl, A., Stammer, D., Henry, O., Cazenave, A., Prandi, P., Knudsen, P., Andersen, O.B., Gao, Y., Johannessen, J., 2014. Multimodel simulations of Arctic Ocean sea surface height variability in the period 1970–2009. J. Geophys. Res. Oceans 119. http://dx.doi.org/10.1002/2014JC010170.

Meyssignac, B., Becker, M., Llovel, W., Cazenave, A., 2012. An assessment of two-dimensional past sea level reconstructions over 1950–2009 based on tide-gauge data and different input sea level grids. Surv. Geophys. 33 (5), 945–972. http://dx.doi.org/10.1007/s10712-011-9171-x.

Nerem, R.S., Leuliette, E., Cazenave, A., 2006. Present-day sea-level change: a review. C.R. Geosci. 338 (14–15), 1077–1083. http://dx.doi.org/10.1016/j.crte.2006.09.001.

Nielsen, A.A. (2013). Least squares adjustment: linear and nonlinear weighted regression analysis. Lecture note, pp. 13–14. <http://www2.imm.dtu.dk/pubdb/views/publicationdetails.php?id=2804>

Peltier, W., 2004. Global glacial isostasy and the surface of the ice-age earth: the ICE-5G (VM2) model and GRACE. Annu. Rev. Earth Planet. Sci. 32, 111–149.

Proshutinsky, A., Ashik, I.M., Dvorkin, E.N., Häkkinen, S., Krishfield, R.A., Peltier, W.R., 2004. Secular sea level change in the Russian sector of the Arctic Ocean. J. Geophys. Res. 109, C03042. http://dx.doi.org/10.1029/2003JC002007.

Permanent Service for Mean Sea Level (PSMSL), 2014, Tide Gauge Data, Retrieved 27 Feb 2013 from <http://www.psmsl.org/data/obtaining/>.

Rosner, B., 1975. On the detection of many outliers. Technometrics 17 (2), 221–227.